Article

Highly Fluorescent Solid-State Asymmetric Spirosilabifluorene Derivatives

Sang Ho Lee, Bo-Bin Jang, and Zakya H. Kafafi

J. Am. Chem. Soc., **2005**, 127 (25), 9071-9078• DOI: 10.1021/ja042762q • Publication Date (Web): 07 June 2005

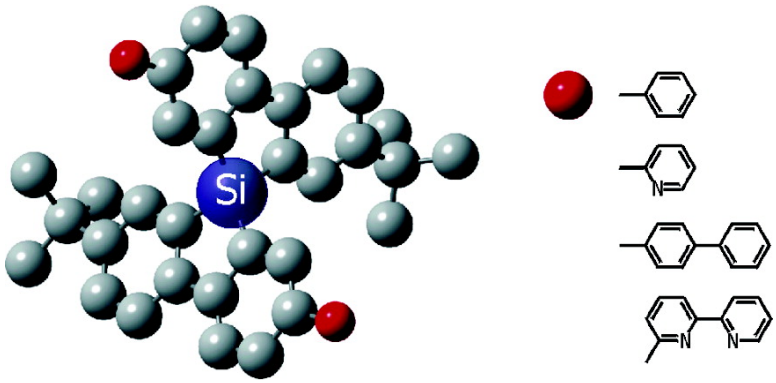

More About This Article

Additional resources and features associated with this article are available within the HTML version:

- Supporting Information
- Links to the 27 articles that cite this article, as of the time of this article download
- Access to high resolution figures
- Links to articles and content related to this article
- Copyright permission to reproduce figures and/or text from this article

View the Full Text HTML

J|A|C|S
ARTICLES
Published on Web 06/07/2005

Highly Fluorescent Solid-State Asymmetric Spirosilabifluorene Derivatives

Sang Ho Lee,*,† Bo-Bin Jang, and Zakya H. Kafafi*

Contribution from the Optical Sciences Division, U.S. Naval Research Laboratory, Washington, D.C. 20375

Received December 1, 2004; E-mail: sangho@ccs.nrl.navy.mil; kafafi@nrl.navy.mil

Abstract: A series of four asymmetrically aryl-substituted 9,9′-spiro-9-silabifluorene (SSF) derivatives, 2,2′-di-*tert*-butyl-7,7′-diphenyl-9,9′-spiro-9-silabifluorene (PhSSF), 2,2′-di-*tert*-butyl-7,7′-dipyridin-2-yl-9,9′-spiro-9-silabifluorene (PySSF), 2,2′-di-*tert*-butyl-7,7′-dibiphenyl-4-yl-9,9′-spiro-9-silabifluorene (BPhSSF), and 2,2′-di-*tert*-butyl-7,7′-bis(2′,2″-bipyridin-6-yl)-9,9′-spiro-9-silabifluorene (BPySSF) are prepared through the cyclization of the corresponding 2,2′-dilithiobiphenyls with silicon tetrachloride. These novel spiro-linked silacyclopentadienes (siloles) form transparent and stable amorphous films with relatively high glass transition temperatures (T_g = 203−228 °C). The absorbance spectrum of each compound shows a significant bathochromic shift relative to that of the corresponding carbon analogue as a result of the effective $\sigma^*-\pi^*$ conjugation between the σ^* orbital of the exocyclic Si−C bond and the π^* orbital of the oligoarylene fragment. Solid-state films exhibit intense violet-blue emission (λ_{PL} = 398−415 nm) with high absolute photoluminescence quantum yields (Φ_{PL} = 30−55%).

Introduction

Spirobifluorenes have been developed and used in organic light-emitting diodes (OLEDs),[1] organic photovoltaic cells (OPVs),[2] optically pumped solid-state lasers,[3] and organic phototransistors[4] and as nonlinear optical (NLO)[5] and photochromic materials.[6] The introduction of a "spiro" linkage into low molecular weight organic compounds results in many advantageous properties, such as high thermal and morphological stabilities, facile processability, and high luminescence quantum efficiencies. In general, spiro-linked molecules consist of two identical (symmetric) or different (asymmetric) molecular units which are orthogonally arranged and connected through a central atom (spiro center).[7] This molecular structure determines their electronic and optical properties. Steric factors can lead to an enhanced rigidity in the spiro center, thereby preventing rotation of the adjacent aryl groups, which reduces close packing and intermolecular interaction between chromophores in the solid state. The spiro-linked molecules compared to the corresponding non-spiro-linked parent compounds exhibit greater morphological stability and more intense fluorescence. These enhanced properties occur without a significant change in their absorption and fluorescence spectra. For example, 2,2,7,7-tetrakis(diphenylamino)-9,9-spirobifluorene (a spiro-TPD analogue for hole transport) shows a high glass transition temperature (T_g = 133 °C), more than double that of *N*,*N*′-diphenyl-*N*,*N*′-(*m*-tolyl)benzidine (TPD) (T_g = 60 °C), while similar electronic and optical properties are maintained.[8]

Silicon-containing π-conjugated compounds, especially silacyclopentadienes (siloles), have emerged as a new class of electroactive materials with intense solid-state fluorescence and/or good electron transport properties in OLEDs.[9−17] Siloles have a relatively low-lying lowest unoccupied molecular orbital (LUMO) level due to the $\sigma^*-\pi^*$ conjugation between the σ^* orbital of the exocyclic Si−C bond and the π^* orbital of the butadiene fragment, resulting in a high electron affinity.[9−11] Recently, a silole derivative, namely, 2,5-bis(2′,2″-

† Also at SFA Inc., Largo, MD 20774.

(1) (a) Salbeck, J.; Yu, N.; Bauer, J.; Weissörtel, F.; Bestgen, H. *Synth. Met.* **1997**, *91*, 209. (b) Steuber, F.; Staudigel, J.; Stössel, M.; Simmerer, J.; Winnacker, A.; Spreitzer, H.; Weissörtel, F.; Salbeck, J. *Adv. Mater.* **2000**, *12*, 130. (c) Wong, K.-T.; Chien, Y.-Y.; Chen, R.-T.; Wang, C.-F.; Lin, Y.-T.; Chiang, H.-H.; Hsieh, P.-Y.; Wu, C.-C.; Chou, C. H.; Su, Y. O.; Lee, G.-H.; Peng, S.-M. *J. Am. Chem. Soc.* **2002**, *124*, 11576. (d) Wu, C. C.; Lin, Y. T.; Chiang, H. H.; Cho, T. Y.; Chen, C. W.; Wong, K. T.; Liao, Y. L.; Lee, G. H.; Peng, S. M. *Appl. Phys. Lett.* **2002**, *81*, 577.
(2) Bach, U.; Lupo, D.; Comte, P.; Moser, J. E.; Weissörtel, F.; Salbeck, J.; Spreitzer, H.; Grätzel, M. *Nature* **1998**, *395*, 583.
(3) (a) Johansson, N.; Salbeck, J.; Bauer, J.; Weissörtel, F.; Bröms, P.; Andersson, A.; Salaneck, W. R. *Adv. Mater.* **1998**, *10*, 1136. (b) Salbeck, J.; Schörner, M.; Fuhrmann, T. *Thin Solid Films* **2002**, *417*, 20.
(4) Saragi, T. P. I.; Pudzich, R.; Fuhrmann, T.; Salbeck, J. *Appl. Phys. Lett.* **2004**, *84*, 2334.
(5) Kim, S. Y.; Lee, M.; Boo, B. H. *J. Chem. Phys.* **1998**, *109*, 2593.
(6) Tian, H.; Chen, B.; Liu, P.-H. *Chem. Lett.* **2001**, 990.
(7) (a) Russell, A. G.; Spencer, N. S.; Philp, D.; Kariuki, B. M.; Snaith, J. S. *Organometallics* **2003**, *22*, 5589. (b) Fournier, J.-H.; Maris, T.; Wuest, J. D. *J. Org. Chem.* **2004**, *69*, 1762.
(8) Salbeck, J.; Weissörtel, F. *Macromol. Symp.* **1997**, *125*, 121.
(9) Tamao, K.; Uchida, M.; Izumizawa, T.; Furukawa, K.; Yamaguchi, S. *J. Am. Chem. Soc.* **1996**, *118*, 11974.
(10) Yamaguchi, S.; Endo, T.; Uchida, M.; Izumizawa, T.; Furukawa, K.; Tamao, K. *Chem. Eur. J.* **2000**, *6*, 1683.
(11) Watkins, N. J.; Mäkinen, A. J.; Gao, Y.; Uchida, M.; Kafafi, Z. H. *Proc. SPIE Int. Soc. Opt. Engr.* **2004**, *5214*, 368.
(12) Palilis, L. C.; Mäkinen, A. J.; Uchida, M.; Kafafi, Z. H. *Appl. Phys. Lett.* **2003**, *82*, 2209.
(13) Palilis, L. C.; Murata, H.; Uchida, M.; Kafafi, Z. H. *Org. Electron.* **2003**, *4*, 113.
(14) Uchida, M.; Izumizawa, T.; Nakano, T.; Yamaguchi, S.; Tamao, K.; Furukawa, K. *Chem. Mater.* **2001**, *13*, 2680.
(15) Murata, H.; Malliaras, G. G.; Uchida, M.; Shen, Y.; Kafafi, Z. H. *Chem. Phys. Lett.* **2001**, *339*, 161.
(16) Murata, H.; Kafafi, Z. H.; Uchida, M. *Appl. Phys. Lett.* **2002**, *80*, 189.
(17) Palilis, L. C.; Uchida, M.; Kafafi, Z. H. *IEEE J. Select. Top. Quan. Electron.* **2004**, *10*, 79.

bipyridin-6-yl)-1,1-dimethyl-3,4-diphenylsilacyclopentadiene (PyPySPyPy), was shown to exhibit nondispersive and air-stable electron transport with a time-of-flight mobility (2.0×10^{-4} cm^2/V s at $E = 0.64$ MV/cm) more than 2 orders of magnitude higher than that of tris(8-hydroxyquinolinato)aluminum(III) (Alq_3), the most commonly used electron-transporting material in OLEDs.[15] In addition, PyPySPyPy formed Ohmic contacts with CsF/Al cathodes, which led to efficient electron injection and space-charged transport in single-layer "electron-only" devices.[17] Theoretical calculations of the electronic and molecular structures of PyPySPyPy revealed a very small dihedral angle (32°) between the silole ring and the bipyridyl moiety, which should give rise to tight packing and strong intermolecular interactions in the solid state.[18] This may facilitate electron hopping between adjacent molecules and explain the superior electron transport properties of PyPySPyPy.

High solid-state photoluminescence quantum yields ($\Phi_{PL} = 30-100\%$) with a high degree of color tunability have been reported upon changing substituents at the 2- and 5-positions on the silole ring.[10,16] The unusually high PL quantum yield of siloles in the solid state has been attributed to aggregation-induced emission (AIE).[19] AIE-active molecules such as the siloles are excellent candidates as light-emitting materials in OLEDs and solid-state lasers. OLEDs based on siloles exhibit excellent performance with external electroluminescence quantum efficiencies ($\eta_{EL} \sim 4.8\%$ at 100 A/m^2) close to the theoretical limit for a fluorescent material and very high brightness (luminance over 10 000 cd/m^2).[12,16] Unfortunately, these siloles easily crystallize due to their low glass transition temperatures. This strong tendency for crystallization contributes to device degradation when these materials are incorporated in OLED structures.

To circumvent this problem, we synthesized a novel class of 9,9′-spiro-9-silabifluorenes (SSFs), which are expected to exhibit high glass transition temperatures and solid-state PL quantum yields. We investigate the effect of adding electron-withdrawing or -donating substituents on the optical and electronic properties of this series of asymmetrically substituted SSFs.

Experimental Section

Measurements. ^1H and ^{13}C NMR spectra were recorded on a Bruker 300 MHz NMR spectrometer using tetramethylsilane (TMS) as the internal reference (0.00 ppm). Column chromatography was performed with 32−63 mesh silica gel. Differential scanning calorimetry (DSC) was carried out on a TA Instruments DSC 2920 differential scanning calorimeter with a scan rate of 20 °C/min. UV/vis spectra were measured on a Hewlett-Packard 8453 spectrophotometer. Fluorescence spectra were obtained with an ISA Fluorolog-3 (JY Horiba) spectrofluorimeter with excitation and emission slit widths set at 1.0 nm. Cyclic voltammetry was performed on a Bioanalytical Systems Inc. model CV-50W potentiostat in a three-electrode cell with a Pt counter electrode, a Ag/AgCl reference electrode, and a glassy carbon working electrode at a scan rate of 100 mV/s with 0.1 M tetrabutylammonium perchlorate as the supporting electrolyte in degassed CH_3CN:THF [9:1 (v/v)] solution purged with argon. At the end of each set of voltammetric experiments, ferrocene (Fc) was added to the solution in order to correct the observed potential with a Fc/Fc^+ reference potential (0.1 V). Mass spectra were recorded on a Finnigan TSQ-70 mass spectrometer. Elemental analyses were performed by Quantitative Technologies Inc. (QTI).

Materials. All commercially available chemicals, reagents, and solvents were used as received without further purification, unless otherwise stated. Tetrahydrofuran (THF) and diethyl ether were distilled over sodium/benzophenone under dry nitrogen. Toluene was distilled over P_2O_5 prior to use. Benzyltrimethylammonium dichloroiodonate ($BTMAICl_2$),[20] tetra-*n*-butylammonium tribromide (Bu_4NBr_3),[21] and 6-(trimethylstannyl)-2,2′-bipyridine[22] were prepared according to published procedures.

3-Bromo-4-iodoaniline (1). To a solution of 3-bromoaniline (2.39 g, 13.9 mmol) in dichloromethane (200 mL) and methanol (80 mL) were added $BTMAICl_2$ (4.84 g, 13.9 mmol) and $CaCO_3$ (1.81 g, 18.1 mmol). The mixture was stirred for 1 h at room temperature until the solution color changed from yellow to light brown. The excess $CaCO_3$ was filtered, and the filtrates were concentrated. The residue was poured into an aqueous solution of $NaHSO_3$ (5%, 70 mL). The mixture was extracted with 50 mL of ethyl acetate, dried over $MgSO_4$, and concentrated to yield a dark brown residue. The crude product was purified by column chromatography (silica gel, hexane/ethyl acetate = 8/1) to afford **1** as a pale yellow oil (3.97 g) in 96% yield. ^1H NMR ($CDCl_3$): δ 7.52 (d, $J = 8.51$ Hz, 1H), 6.99 (s, 1H), 6.37−6.33 (dd, $J = 8.68$, 2.66 Hz, 1H), 3.73 (s, 1H). ^{13}C NMR ($CDCl_3$): δ 147.5, 140.1, 129.8, 118.9, 115.8.

***N*-(3-Bromo-4-iodophenyl)acetamide (2).** To a solution of 3-bromo-4-iodoaniline (3.50 g, 11.7 mmol) in acetic anhydride (12 mL) was added a catalytic amount of H_2SO_4. The mixture was stirred for 20 min at room temperature. The solution was neutralized with 100 mL of saturated aqueous sodium carbonate and extracted with 150 mL of ethyl acetate. The organic layer was washed with water (100 mL) and brine (70 mL), dried over $MgSO_4$, and concentrated. The crude solid was recrystalized from chloroform to afford **2** as a white solid (3.95 g). ^1H NMR ($CDCl_3$): δ 7.88 (s, 1H), 7.73 (d, $J = 8.66$ Hz, 1H), 7.60 (s, 1H), 7.19−7.16 (dd, $J = 8.54$, 2.36 Hz, 1H), 2.17 (s, 3H). ^{13}C NMR ($CDCl_3$): δ 169.0, 140.1, 138.9, 129.8, 123.8, 120.0, 94.3, 24.5.

2-Bromo-4-*tert*-butylaniline (3). To a solution of 4-*tert*-butylaniline (4.07 g, 27.0 mmol) in 70 mL of DMF:H_2O [7:3 (v/v)] was added slowly Bu_4NBr_3 (13.2 g, 27.0 mmol) in 10 mL of DMF at 0 °C. The mixture was stirred for 10 min at a temperature of 0−5 °C. The residue was poured into an aqueous solution of $NaHSO_3$ (5%, 200 mL). The mixture was extracted with 70 mL of ethyl acetate, dried over $MgSO_4$, and concentrated to yield a dark brown oil. The crude product was purified by column chromatography (silica gel, hexane) to afford **3** as a pale yellow oil (4.00 g) in 64% yield. ^1H NMR ($CDCl_3$): δ 7.40 (s, 1H), 7.13−7.10 (dd, $J = 8.45$, 2.20 Hz, 1H), 6.69 (d, $J = 8.36$ Hz, 1H), 3.85 (s, 2H), 1.25 (s, 9H).

2-Bromo-4-*tert*-butyl-1-iodobenzene (4). To a solution of 2-bromo-4-*tert*-butylaniline (10.6 g, 46.5 mmol) in concentrated H_2SO_4 (25 mL) and H_2O (230 mL) was slowly added sodium nitrite (4.17 g, 60.4 mmol) in H_2O (10 mL) at 5 °C. The resulting solution was stirred for 2 h at 10 °C and then slowly added into a vigorously stirred solution of KI (61.9 g, 0.37 mol) in 150 mL of H_2O at 5 °C. The mixture was stirred at room temperature for 6 h, followed by reflux for 20 min. The residue was poured into an aqueous solution of $NaHSO_3$ (5%, 300 mL) and then stirred for 20 min at room temperature. The mixture was extracted with 250 mL of ethyl acetate, dried over $MgSO_4$, and concentrated to yield a brown oil. The crude product was purified by column chromatography (silica gel, hexane) to afford **4** as a colorless oil (12.5 g) in 79% yield. ^1H NMR ($CDCl_3$): δ 7.71 (d, $J = 8.32$ Hz, 1H), 7.61 (s, 1H), 7.00−6.96 (dd, $J = 8.43$, 2.36 Hz, 1H), 1.25 (s, 9H). ^{13}C NMR ($CDCl_3$): δ 153.3, 139.7, 130.0, 129.5, 125.9, 97.1, 34.6, 31.0.

(18) Risko, C.; Kushto, G. P.; Kafafi, Z. H.; Brédas, J. L. *J. Chem. Phys.* **2004**, *121*, 9031; ibid, **2005**, *122*, 099901.
(19) Chen, J.; Law, C. C. W.; Lam, J. W. Y.; Dong, Y.; Lo, S. M. F.; Williams, I. D.; Zhu, D.; Tang, B. Z. *Chem. Mater.* **2003**, *15*, 1535.
(20) Kajigaeshi, S.; Kakinami, T.; Yamasaki, H.; Fujisaki, S.; Okamoto, T. *Bull. Chem. Soc. Jpn.* **1988**, *61*, 600.
(21) Tidwell, J. H.; Buchwald, S. L. *J. Am. Chem. Soc.* **1994**, *116*, 11797.
(22) Cardenas, D. J.; Sauvage, J. P. *Synlett* **1996**, *9*, 916.

2-(2-Bromo-4-*tert*-butylphenyl)-4,4,5,5-tetramethyl-1,3,2-dioxaborolane (5). To a solution of 2-bromo-4-*tert*-butyl-1-iodobenzene (7.87 g, 23.0 mmol) in 150 mL of THF was slowly added *i*-PrMgBr (11.6 mL of a 2 M solution in THF, 23.0 mmol) at −40 °C. The resulting solution was stirred for 2 h at −40 °C. Subsequently, 2-isopropoxy-4,4,5,5-tetramethyl-1,3,2-dioxaborolane (6.98 g, 37.0 mmol) was added rapidly to the resulting intermediate at −40 °C. The mixture was allowed to warm up to room temperature slowly and then further stirred for 5 h. The organic mixture was extracted with 200 mL of ethyl acetate, washed with 150 mL of H_2O, dried over $MgSO_4$, and concentrated to yield a colorless oil. The crude product was purified by column chromatography (silica gel, hexane/chloroform = 5/1) to afford **5** as a colorless oil (5.58 g) in 71% yield. ^{1}H NMR ($CDCl_3$): δ 7.58−7.55 (m, 2H), 7.31−7.27 (dd, J = 7.83, 1.67 Hz, 1H), 1.36 (s, 12H), 1.29 (s, 9H). ^{13}C NMR ($CDCl_3$): δ 155.7, 136.4, 129.8, 123.4, 84.0, 34.8, 30.9, 24.7.

***N*-(2,2′-Dibromo-4′-*tert*-butylbiphenyl-4-yl)acetamide (6).** 2-(2-Bromo-4-*tert*-butylphenyl)-4,4,5,5-tetramethyl-1,3,2-dioxaborolane (10.0 g, 29.5 mmol), *N*-(3-bromo-4-iodophenyl)acetamide (13.1 g, 38.5 mmol), $Pd(PPh_3)_4$ (0.89 g, 0.77 mmol), and CsF (4.50 g, 29.6 mmol) were added to a round-bottom flask equipped with a stir bar. The round-bottom flask was capped with a septum and then evacuated. To the reaction mixture was added 170 mL of THF via cannula and refluxed for 24 h. The reaction mixture was then diluted with ethyl acetate (300 mL), washed with brine (200 mL), dried over $MgSO_4$, and concentrated to yield a tan solid. The crude product was purified by column chromatography (silica gel, hexane/ethyl acetate = 4/1) to afford **6** as a white solid (10.8 g) in 86% yield. ^{1}H NMR ($CDCl_3$): δ 7.89 (s, 1H), 7.64 (s, 1H), 7.62 (s, 1H), 7.53−7.50 (dd, J = 8.29, 2.06 Hz, 1H), 7.38−7.34 (dd, J = 8.15, 2.06 Hz, 1H), 7.17 (d, J = 8.36 Hz, 1H), 7.14 (d, J = 8.07, 1H), 2.21 (s, 3H), 1.35 (s, 9H). ^{13}C NMR ($CDCl_3$): δ 167.2, 150.9, 138.4, 136.9, 134.5, 129.5, 129.3, 127.5, 122.7, 121.7, 121.4, 121.0, 116.4, 33.0, 29.5, 22.6. Anal. Calcd for $C_{18}H_{19}Br_2NO$: C, 50.85; H, 4.50; N, 3.29. Found: C, 50.82; H, 4.23; N, 3.24.

2,2′-Dibromo-4-*tert*-butyl-4′-iodobiphenyl (7). A solution of *N*-(2,2′-dibromo-4′-*tert*-butylbiphenyl-4-yl)acetamide (2.87 g, 6.80 mmol) in ethanol (10 mL) and concentrated HCl (10 mL) was refluxed for 1 h and then evaporated in vacuo. To an amine solution in 2 N HCl (50 mL) and THF (5 mL) was slowly added sodium nitrite (0.61 g, 8.80 mmol) in H_2O (3 mL) at 5 °C. The resulting solution was stirred for 2 h at 10 °C and then slowly added into a vigorously stirred solution of KI (8.90 g, 53.6 mmol) in 100 mL of H_2O at 5 °C. The mixture was stirred at room temperature for 6 h, followed by reflux for 20 min. The residue was poured into an aqueous solution of $NaHSO_3$ (5%, 150 mL) and then stirred for 20 min at room temperature. The mixture was extracted with 200 mL of ethyl acetate, dried over $MgSO_4$, and concentrated to yield a dark brown residue. The crude product was purified by column chromatography (silica gel, hexane) to afford **7** as a colorless oil (2.41 g) in 72% yield. ^{1}H NMR ($CDCl_3$): δ 8.01 (s, 1H), 7.69−7.64 (m, 2H), 7.38−7.35 (dd, J = 8.06, 1.85 Hz, 1H), 7.12 (d, J = 8.09 Hz, 1H), 6.96 (d, J = 8.04 Hz, 1H), 1.34 (s, 9H). ^{13}C NMR ($CDCl_3$): δ 153.2, 141.6, 140.5, 138.0, 136.1, 132.5, 130.3, 129.6, 124.6, 124.3, 122.9, 93.5, 34.7, 31.1. Anal. Calcd for $C_{16}H_{15}Br_2I$: C, 38.90; H, 3.06. Found: C, 38.82; H, 2.93.

2,2′-Dibromo-4-*tert*-butyl-[1,1′;4′,1″]terphenyl (8a). To a solution of 2,2′-dibromo-4-*tert*-butyl-4′-iodobiphenyl (0.92 g, 1.86 mmol) in toluene (50 mL) and aqueous saturated $Ba(OH)_2$ (30 mL) were added 2-phenylboronic acid (0.27 g, 2.23 mmol) and $Pd(PPh_3)_4$ (21.5 mg, 0.02 mmol). The reaction mixture was refluxed for 12 h and then diluted with ethyl acetate (100 mL). The organic mixture was washed with brine, dried over $MgSO_4$, and concentrated to yield a crude solid. The crude product was purified by column chromatography (silica gel, hexane) to afford **8a** as a white solid (0.68 g) in 83% yield. ^{1}H NMR (CD_2Cl_2): δ 7.92 (s, 1H), 7.71 (s, 1H), 7.67−7.61 (m, 3H), 7.51−7.41 (m, 4H), 7.32 (d, J = 8.03 Hz, 1H), 7.22 (d, J = 7.90, 1H), 1.37 (s, 9H).

2-(2,2′-Dibromo-4′-*tert*-butylbiphenyl-4-yl)pyridine (8b). To a solution of 2,2′-dibromo-4-*tert*-butyl-4′-iodobiphenyl (1.24 g, 2.51 mmol) in toluene (50 mL) were added 2-tributylstannylpyridine (1.02 g, 2.76 mmol) and $Pd(PPh_3)_4$ (96.0 mg, 0.08 mmol). The reaction mixture was refluxed for 12 h and then diluted with ethyl acetate (100 mL). The organic mixture was washed with brine, dried over $MgSO_4$, and concentrated to yield a crude solid. The crude product was purified by column chromatography (silica gel, hexane/ethyl acetate = 7/1) to afford **8b** as a white solid (1.06 g) in 95% yield. ^{1}H NMR ($CDCl_3$): δ 8.68 (d, J = 4.93 Hz, 1H), 8.34 (s, 1H), 7.97−7.94 (dd, J = 8.18, 1.73 Hz, 1H), 7.72−7.67 (m, 3H), 7.39−7.36 (dd, J = 8.18, 2.03 Hz, 1H), 7.32 (d, J = 7.88 Hz, 1H), 7.23−7.17 (m, 2H), 1.34 (s, 9H). ^{13}C NMR ($CDCl_3$): δ 155.3, 152.8, 149.6, 142.2, 140.3, 138.5, 136.8, 131.4, 130.8, 130.4, 129.4, 125.3, 124.1, 123.0, 122.6, 120.4, 34.6, 31.1.

2,2′-Dibromo-4-*tert*-butyl-[1,1′;4′,1″;4″,1‴]quaterphenyl (8c). To a solution of 2,2′-dibromo-4-*tert*-butyl-4′-iodobiphenyl (1.10 g, 2.23 mmol) in toluene (50 mL) and aqueous saturated $Ba(OH)_2$ (30 mL) were added 2-biphenylboronic acid (0.46 g, 2.23 mmol) and $Pd(PPh_3)_4$ (26.0 mg, 0.02 mmol). The reaction mixture was refluxed for 12 h and then diluted with ethyl acetate (100 mL). The organic mixture was washed with brine, dried over $MgSO_4$, and concentrated to yield a crude solid. The crude product was purified by column chromatography (silica gel, petroleum ether) to afford **8c** as a white solid (0.91 g) in 79% yield. ^{1}H NMR ($CDCl_3$): δ 7.95 (s, 1H), 7.70−7.62 (m, 8H), 7.50−7.37 (m, 4H), 7.33 (d, J = 7.89 Hz, 1H), 7.22 (d, J = 8.00 Hz, 1H), 1.37 (s, 9H). ^{13}C NMR ($CDCl_3$): δ 152.8, 141.7, 140.7, 140.6, 140.2, 138.6, 137.9, 131.4, 130.7, 130.6, 129.5, 128.8, 127.5, 127.4, 127.3, 126.9, 125.5, 124.2, 124.1, 123.2, 34.6, 31.1.

6-(2,2′-Dibromo-4′-*tert*-butylbiphenyl-4-yl)[2,2′]bipyridinyl (8d). To a solution of 2,2′-dibromo-4-*tert*-butyl-4′-iodobiphenyl (2.40 g, 4.86 mmol) in toluene (120 mL) were added 6-(trimethylstannyl)-2,2′-bipyridine (2.01 g, 6.30 mmol) and $Pd(PPh_3)_4$ (0.19 g, 0.16 mmol). The reaction mixture was refluxed overnight and then diluted with ethyl acetate (150 mL). The organic mixture was washed with brine, dried over $MgSO_4$, and concentrated to yield a crude solid. The crude product was purified by column chromatography (silica gel, hexane/ethyl acetate = 7/1) to afford **8d** as a pale yellow solid (1.73 g) in 68% yield. ^{1}H NMR ($CDCl_3$): δ 8.71−8.69 (m, 1H), 8.65 (d, J = 7.83 Hz, 1H), 8.49 (s, 1H), 8.42 (d, J = 7.49 Hz, 1H), 8.14−8.11 (dd, J = 8.11, 1.70 Hz, 1H), 7.95−7.79 (m, 3H), 7.69 (s, 1H), 7.43−7.32 (m, 3H), 7.22 (d, J = 8.10 Hz, 1H), 1.38 (s, 9H). ^{13}C NMR ($CDCl_3$): δ 155.9, 155.8, 154.4, 152.9, 149.0, 142.4, 140.3, 138.7, 137.8, 136.8, 131.4, 130.9, 130.5, 129.6, 129.5, 125.4, 124.2, 123.8, 123.1, 121.2, 120.2, 119.8, 34.7, 31.2.

2,2′-Di-*tert*-butyl-7,7′-diphenyl-9,9′-spiro-9-silabifluorene (9a). To a solution of 2,2′-dibromo-4-*tert*-butyl-[1,1′;4′,1″]terphenyl (3.92 g, 8.82 mmol) in diethyl ether (200 mL) at −78 °C was added *n*-BuLi (11.0 mL of 1.6 M in hexane, 17.6 mmol). The reaction solution was allowed to warm to room temperature and stirred for 6 h. Silicon tetrachloride (0.72 g, 4.23 mmol) in 10 mL of diethyl ether was added to the resulting solution at room temperature. The reaction mixture was stirred at room temperature for 1.5 h and refluxed for 3 h. A yellow solution and a white precipitate were obtained. The residue was washed with H_2O, dried over $MgSO_4$, and concentrated to yield a crude solid. The crude product was purified by column chromatography (silica gel, hexane/ethyl acetate = 27/1) to afford **9a** as a white solid (1.92 g) in 73% yield. ^{1}H NMR (CD_2Cl_2): δ 8.00 (d, J = 8.12 Hz, 1H), 7.93 (d, J = 8.21 Hz, 1H), 7.77−7.74 (dd, J = 8.09, 1.88 Hz, 1H), 7.64 (s, 1H), 7.61−7.58 (dd, J = 8.18, 1.98 Hz, 1H), 7.56−7.50 (m, 3H), 7.37−7.23 (m, 3H), 1.27 (s, 9H). ^{13}C NMR (CD_2Cl_2): δ 151.5, 149.5, 147.6, 140.9, 140.5, 134.3, 133.1, 133.0, 131.4, 130.4, 129.2, 129.0, 127.6, 127.1, 121.6, 121.3, 35.1, 31.5. Anal. Calcd for $C_{44}H_{40}Si$: C, 88.54; H, 6.75. Found: C, 88.23; H, 6.58.

2,2′-Di-*tert*-butyl-7,7′-dipyridin-2-yl-9,9′-spiro-9-silabifluorene (9b). **9b** was synthesized using the same procedure described above for

Scheme 1. Synthesis of Asymmetrically Substituted Spirosilabifluorenes

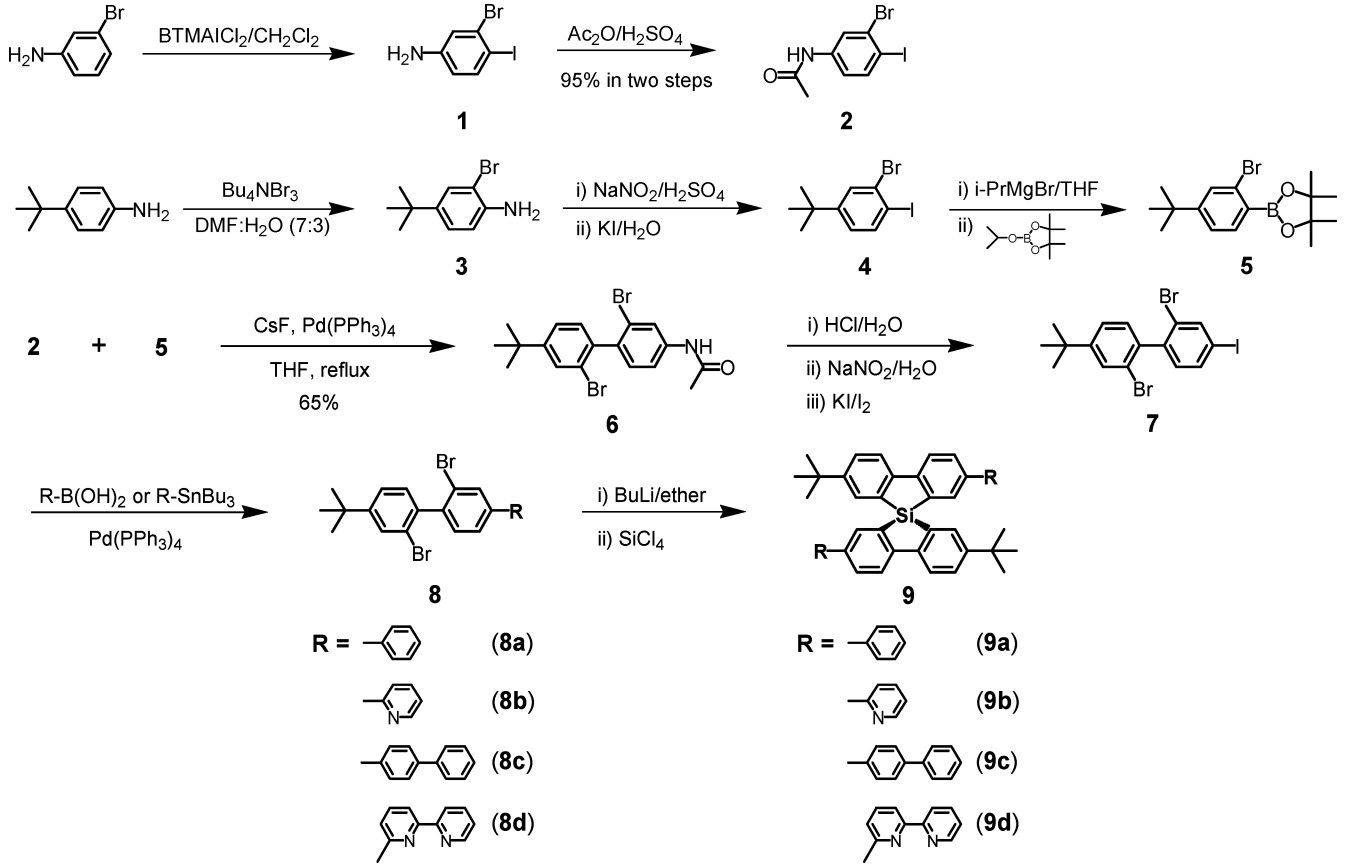

9a. A pale yellow solid was obtained in 68% yield. ^{1}H NMR ($CDCl_3$): δ 8.60−8.58 (m, 1H), 8.17−8.13 (dd, J = 8.26, 1.58 Hz, 1H), 8.03−8.00 (m, 2H), 7.94 (d, J = 8.23 Hz, 1H), 7.68−7.64 (m, 2H), 7.61−7.58 (dd, J = 8.26, 2.08 Hz, 1H), 7.51 (s, 1H), 7.16−7.11 (m, 1H), 1.27 (s, 9H). ^{13}C NMR ($CDCl_3$): δ 157.1, 151.2, 150.7, 149.5, 147.1, 138.3, 136.6, 133.6, 133.0, 132.7, 131.3, 130.0, 128.7, 121.9, 121.1, 121.0, 120.5, 34.9, 31.3. Anal. Calcd for $C_{42}H_{38}N_2Si$: C, 84.24; H, 6.40; N, 4.68. Found: C, 83.84; H, 6.17; N, 4.71.

2,2′-Di-*tert*-butyl-7,7′-dibiphenyl-4-yl-9,9′-spiro-9-silabifluorene (9c). 9c was synthesized using the same procedure described above for **9a**. A white solid was obtained in 65% yield. ^{1}H NMR (CD_2Cl_2): δ 8.03 (d, J = 8.15, 1H), 7.95 (d, J = 8.17 Hz, 1H), 7.84−7.81 (dd, J = 8.18, 2.10 Hz, 1H), 7.72 (s, 1H), 7.67−7.59 (m, 7H), 7.52 (s, 1H), 7.44−7.39 (m, 2H), 7.35−7.32 (m, 1H), 1.30 (s, 9H). ^{13}C NMR (CD_2Cl_2): δ 150.9, 149.0, 147.0, 140.3, 139.7, 139.3, 133.7, 132.5, 132.4, 131.0, 129.6, 128.6, 128.5, 127.1, 126.9, 126.7, 121.0, 120.6, 34.6, 31.0. Anal. Calcd for $C_{56}H_{48}Si$: C, 89.79; H, 6.46. Found: C, 89.22; H, 6.42.

2,2′-Di-*tert*-butyl-7,7′-bis(2′,2″-bipyridin-6-yl)-9,9′-spiro-9-silabifluorene (9d).[23] **9d** was synthesized using the same procedure described above for **9a**. A pale yellow solid was obtained in 1% yield. ^{1}H NMR (CD_2Cl_2): δ 8.64−8.62 (m, 1H), 8.55−8.52 (m, 1H), 8.43−8.40 (dd, J = 8.23, 2.03 Hz, 1H), 8.32−8.29 (dd, J = 7.69, 1.02 Hz, 1H), 8.14−8.10 (m, 2H), 8.01 (d, J = 8.29, 1H), 7.83−7.71 (m, 3H), 7.65−7.62 (dd, J = 8.15, 1.96 Hz, 1H), 7.53 (s, 1H), 7.32−7.27 (m, 1H), 1.28 (s, 9H). ^{13}C NMR ($CDCl_3$): δ 156.3, 156.2, 155.6, 151.3, 150.8, 148.9, 147.2, 138.5, 137.6, 136.9, 133.4, 133.2, 132.7, 131.3, 130.4, 128.8, 123.7, 121.4, 121.2, 121.0, 120.5, 119.2, 34.9, 31.3.

(23) Due to the extremely low product yield (~1%) of BPySSF **9d**, we could not collect enough highly pure BPySSF **9d** (purified by column chromatography, followed by sequential train sublimation).

Results and Discussion

Synthesis. Aryl-substituted asymmetric spirosilabifluorene (SSF) derivatives were synthesized using the method developed by Gilman:[24] lithiation of substituted 2,2′-dibromobiphenyls **8**, followed by spirocyclization with silicon tetrachloride (Scheme 1). Functionalized 2,2′-dibromobiphenyls **8** were obtained from a single key building block, asymmetric 2,2′-dibromobiphenyl amide **6**. The *tert*-butyl group was introduced to ensure the solubility of the resulting spiro-linked siloles and to provide steric hindrance leading to solid-state amorphous films. We have employed two different methods for the synthesis of asymmetric biphenyl **6**. The first method (not shown) involved conventional Sandmeyer reaction[25] from 2,2′-diaminobiphenyl to 2,2′-dibromobiphenyl, which resulted in low chemical yields (5−7%) due to the poor solubility of the products in acidic media. The second route was based on palladium-catalyzed Suzuki cross-coupling as depicted in Scheme 1. The synthesis of 1-bromo-2-iodobenzene amide **2** was a straightforward (two steps) procedure using readily available starting material, 3-bromoaniline, with a high chemical yield (95%). Iodination of 3-bromoaniline was accomplished by treatment with benzyltrimethylammonium dichloroiodate ($BTMAICl_2$) followed by acetylation with acetic anhydride. The other precursor for the Suzuki coupling was prepared by bromination of 4-*tert*-butylaniline with tetrabutylammonium tribromide (Bu_4NBr_3) in DMF:H_2O [7:3 (v/v)] to yield 2-bromo-4-*tert*-butylaniline **3**, which was then converted to

(24) Gilman, H.; Gorsich, R. D. *J. Am. Chem. Soc*. **1958**, *80*, 1883.
(25) Furniss, B. S.; Hannaford, A. J.; Smith, P. W. G.; Tatchell, A. R. *Vogel's Textbook of Practical Organic Chemistry*, 5th ed.; John Wiley and Sons: New York, 1989.

2-bromo-4-*tert*-butyl-1-iodobenzene **4** via Sandmeyer reaction. Chemoselective I−Mg exchange[26] of 2-bromo-4-*tert*-butyl-1-iodobenzene **4** with a Grignard reagent, *i*-PrMgBr, proceeded smoothly under mild reaction conditions. Subsequent reaction with 2-isopropoxy-4,4,5,5-tetramethyl-1,3,2-dioxaborolane gave 2-bromobenzene boronate **5** in good yield (71%).

We initially used a general palladium-catalyzed Suzuki cross-coupling of iodobenzene **2** with boronate **5** using a mixture of basic aqueous solution (e.g., aq. Na_2CO_3 or aq. K_2CO_3) and organic solvents (THF or toluene) to make 2,2-dibromobiphenyl **6**. Although the isolated product could be obtained in high purity, the low product yield and difficulty of purification prompted us to consider alternative synthetic routes. We have found that palladium-catalyzed coupling of 2-bromobenzene boronate **5** is in competition with the base-catalyzed protodeboronation[27] of the boronic entity in aqueous solution. To address this problem, we selected nonaqueous Suzuki cross-coupling[28] using CsF as a base, which is soluble in organic solvents (e.g. THF, toluene or dioxane) and provides relatively weak basicity and poor nucleophilicity. This approach proved useful in synthesizing asymmetric 2,2′-dibromobiphenyl **6**, because the reaction proceeded selectively, and could be used with a variety of functional groups and led to reasonably high chemical yields (86%).

Biphenyl **6** was converted into 4-amino-4′-*tert*-butyl-2,2′-dibromobiphenyl via hydrolysis, followed by Sandmeyer reaction to afford 4-*tert*-butyl-4′-iodo-2,2′-dibromobiphenyl **7** in good yield (73%). Subsequent selective palladium-catalyzed Suzuki or Stille coupling of 2,2′-dibromo-4-iodobiphenyl **7** with aryl boronic acids or aryl tin derivatives successfully provided functionalized 2,2′-dibromobiphenyls **8** in high yields (68−85%). The series of asymmetric SSFs was purified by column chromatography followed by sequential train sublimation under high vacuum ($\sim 10^{-6}$ Torr). The purity and chemical structures of these compounds were confirmed by ^{1}H NMR, ^{13}C NMR, and elemental analysis.

Thermal Properties. The glass transition temperatures (T_g) of asymmetric SSFs were determined by differential scanning calorimetry (DSC) in a nitrogen atmosphere. A heating rate of 20 °C/min was used after first melting the compound and subsequent rapid cooling to room temperature under ambient conditions. The T_g of symmetric SSF, 2,2′,7,7′-tetra-*tert*-butyl-9,9′-spiro-9-silabifluorene (tBSSF), was also measured and compared to those of asymmetric SSFs in order to investigate the effect of introducing an asymmetric functionality on the SSF ring, in particular with regard to its thermal and morphological stability. The crystalline sample of asymmetric PhSSF **9a**, purified by vacuum sublimation, melted at 314 °C to give isotropic liquids upon heating during the first scan and then changed into a glassy state upon cooling. As shown in Figure 1, when the amorphous glassy sample was heated again, a quite high T_g of 203 °C was observed. In contrast, no glass transition temperature was determined for the unmodified symmetric 9,9′-spiro-9-silabifluorene,[29] which is easily crystallized at room temperature. This suggests that the introduction of both the *tert*-butyl and phenyl groups on the SSF molecule gives rise to an increase in the number of conformers and steric hindrance. The asymmetric substitution coupled with the nonplanar molecular structure leads to the dramatic increase in morphological stability. In addition, this value is 125 °C higher than that of the air-stable electron transporter PyPySPyPy (T_g = 77 °C),[14] demonstrating the superior morphological stability of asymmetric PhSSF **9a**, which we attribute to the spiro-linked bifluorene moiety. Further heating above the glass transition temperature resulted in the appearance of exothermic peaks due to crystallization at 239 °C. This phenomenon is commonly observed in organic materials.

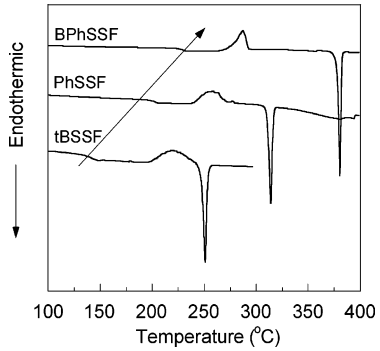

Figure 1. Differential scanning calorimetric (DSC) thermograms of tBSSF, PhSSF, and BPhSSF measured in a dry nitrogen atmosphere at a heating rate of 20 °C/min.

Table 1. Thermal Properties of Asymmetric Spirosilabifluorenes

compd	T_m (°C)	T_g (°C)	compd	T_m (°C)	T_g (°C)
PhSSF	314	203	BPhSSF	382	228
PySSF	334	203	tBSSF	248	141

Asymmetric PySSF **9b** exhibited a melting point of 334 °C and a T_g of 203 °C, respectively, which are similar to those for PhSSF **9a** (Table 1). Asymmetric BPhSSF **9c** exhibited a quite high T_g of 228 °C, which is 25 °C higher than those of asymmetric PhSSF **9a** and PySSF **9b**, and 87 °C higher than that of symmetric tBSSF (T_g = 141 °C). This result suggests that the improved morphological stability of asymmetric BPhSSF **9c** results from an increase in molecular weight and volume. The T_gs of asymmetric SSFs increase linearly with the molecular weight of substituent incorporated into SSF moiety, as illustrated in Figure 1. This relationship thus may be useful in estimating the T_gs of asymmetric SSFs. As a result, we predict that BPySSF **9d** has a T_g higher than that of PySSF **9b**. It should be also noted that amorphous neat films ($\sim$300 nm) of asymmetric SSFs prepared by vacuum vapor deposition onto quartz do not show any sign of crystallization in ambient atmosphere.

Optical Properties. The optical properties of asymmetric SSFs were measured both in chloroform solutions and in neat solid-state films.

(a) In Chloroform Solutions. The normalized absorbance and photoluminescence (PL) spectra of asymmetric SSFs in chloroform solutions measured at room temperature are shown in Figure 2. Their photophysical properties are summarized in Table 2. The absorbance spectrum of asymmetric PhSSF **9a** is characterized by a strong absorption peak centered around 307 nm with a weak shoulder at 347 nm. This spectrum should be similar to that of 2-*tert*-butyl-7-phenylsilafluorene due to the

(26) Poirier, M.; Chen, F.; Bernard, C.; Wong, Y.-S.; Wu, G. G. *Org. Lett.* **2001**, *3*, 3795.
(27) (a) Kuivila, H. G.; Reuwer, J. F.; Mangravite J. A. *J. Am. Chem. Soc.* **1964**, *86*, 2666. (b) Muller, D.; Fleury, J.-P. *Tetrahedron Lett.* **1991**, *32*, 2229.
(28) Wright, S. W.; Hageman, D. L.; McClure, L. D. *J. Org. Chem.* **1994**, *59*, 6095.
(29) Lee, S. H.; Kafafi, Z. H. *Am. Chem. Soc. Org. Prepr.* **2002**, *224*, 490.

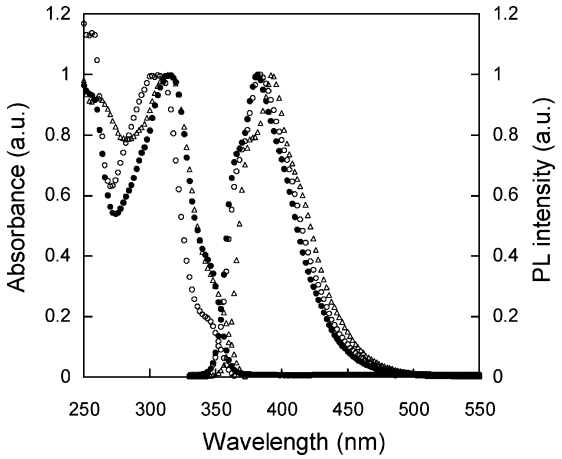

Figure 2. Normalized absorbance and photoluminescence spectra of PhSSF (open circles), BPhSSF (open triangles), and PySSF (closed circles) in chloroform solutions.

Table 2. Photophysical Properties of Asymmetric Spirosilabifluorenes

	λ_{abs} (nm)		λ_{PL} (nm)			
compd	$CHCl_3$	film[b]	$CHCl_3$	film[b]	$\Phi_{PL,film}$[a]	E_g^{opt} (eV)[c]
PhSSF	307	304	383	398	0.44	3.38
PySSF	317	313	382	415	0.31	3.39
BPhSSF	315	318	393	410	0.54	3.29

[a] Determined using an integrating sphere. [b] Neat films prepared by vacuum deposition on quartz substrates (thickness ~300 nm). [c] Estimated from the tail of the absorption spectra.

tetrahedral bonding arrangement around the silicon atom and the lack of any π-conjugation. The latter should be identical to that of 2-phenylsilafluorene as a result of the weak inductive effect of the *tert*-butyl group. Similarly, the optical properties of 2,2′-diphenylspirobifluorene, the carbon analogue of asymmetric PhSSF **9a**, are expected to be analogous to those of 2-phenylfluorene. Hence, one may compare the optical spectrum of PhSSF **9a** to that of 2-phenylfluorene. The maximum peak observed for asymmetric PhSSF **9a** exhibits a significant red shift relative to that of 2-phenylfluorene (λ_{max} = 287 nm),[30] suggesting strong $\sigma^*-\pi^*$ conjugation between the σ^* orbital of the exocyclic Si−C bond and the π^* orbital of the *p*-terphenyl moiety in asymmetric PhSSF **9a**. This observation is consistent with a recent study on the distinct photophysical properties observed for 7-sila-7,7-dimethyl-7*H*-dibenzo[*c*,*g*]fluorene (e.g., bathochromic shifts in both absorbance and fluorescence spectra) relative to those of the corresponding acyclic analogues.[31] When compared to that of tBSSF (λ_{abs} = 287 and 337 nm),[29] the optical absorption of PhSSF **9a** is bathochromically shifted by 10−20 nm, indicating that the phenyl substituent plays a role in determining the gap between the highest occupied molecular orbital (HOMO) and the lowest unoccupied molecular orbital (LUMO). Comparing the absorbance spectra of PySSF **9b** and BPhSSF **9c** to that of PhSSF **9a**, the former showed a slight red shift (8−10 nm) in the lowest energy electronic transition.

Upon excitation at 320 nm, asymmetric PhSSF **9a** showed an intense violet-blue emission centered at 383 nm (Figure 2),

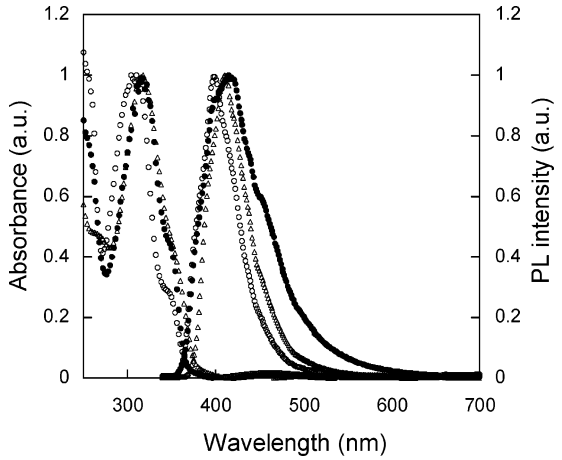

Figure 3. Normalized absorbance and photoluminescence spectra of neat solid-state films of PhSSF (open circles), BPhSSF (open triangles), and PySSF (closed circles).

which is significantly red-shifted relative to that of 2-phenylfluorene (λ_{em} = 343 and 329 nm),[30] reflecting the important role played by silicon in the modified silacyclopentadiene ring. A larger bathochromic shift can be also obtained by lengthening the conjugated system with the addition of a phenyl group to the 9-silafluorene ring. A bathochromic shift of 10 nm was indeed observed for BPhSSF **9c** compared to that for PhSSF **9a**, yielding an intense violet-blue emission with a maximum centered at 393 nm. On the other hand, the electron-accepting pyridyl groups in PySSF **9b** showed no significant influence on its PL spectrum, suggesting that the inductive effect of the pyridyl groups may be counterbalanced by the extended π-conjugation due to the reduced ortho−ortho hydrogen interaction between the silole core and the pyridine unit. Considering that the PL spectra of previously studied 2,5-diaryl-3,4-diphenylsiloles strongly depend on the nature of aryl groups at the 2- and 5-positions,[10] all three asymmetric SSFs do not show significant spectral changes because the electronic interaction is minimal between the silicon atom and the substituents on the 9-silafluorene ring. The observed Stokes shifts were measured to be 6464 cm^{-1} (0.80 eV) for PhSSF **9a**, 5368 cm^{-1} (0.67 eV) for PySSF **9b**, and 6301 cm^{-1} (0.78 eV) for BPhSSF **9c**. In asymmetric SSFs, the aryl-substituted 9-silafluorene may be considered as a modified *p*-oligophenylene in which the single bonds between the phenyl rings have double bond character, i.e. more planar configuration in the excited state.[32] Nonplanar configuration of aryl-substituted 9-silafluorene in the ground state may differ from its excited-state geometry (more planar configuration), leading to the large Stokes shifts between the absorption and emission spectra.

(b) Neat Solid-State Films. As shown in Figure 3, the absorbance spectra of neat solid-state films of asymmetric SSFs are very similar to those measured in chloroform solutions, suggesting that these are true molecular solids with minimal intermolecular interactions in the solid state. The optical band gaps (E_g^{opt}) of the asymmetric SSFs determined from the onset of the solid-state absorbance spectra are summarized in Table 2. All three asymmetric SSFs have optical band gaps in the range 3.29 to 3.39 eV. The PL spectra of the three SSFs in

(30) Berlman, I. B. *J. Chem. Phys.* **1970**, *52*, 5616.
(31) Hoshi, T.; Tomonobu, N.; Suzuki, T.; Ando, M.; Hagiwara, H. *Organometallics* **2000**, *19*, 4483.
(32) Berlman, I. B. *Handbook of Fluorescence Spectra of Aromatic Molecules*, 2nd ed.; Academic Press: New York, 1971.

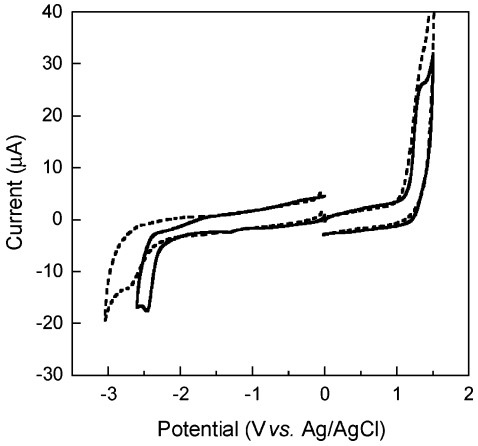

Figure 4. Cyclic voltammograms of BPhSSF (dashed line) and PySSF (solid line) measured in CH_3CN:THF [9:1 (v/v)] at a scan rate of 100 mV/s.

solution are almost identical, whereas a significant broadening in the solid-state PL spectrum of PySSF **9b** is observed. This behavior suggests that the excited-state geometry of PySSF **9b** may favor an effective coplanar configuration in the solid state, which is a result of the small dihedral angle[18] between the ortho-hydrogen-free pyridine and the 9-silafluorene ring, allowing better π orbital overlap. However, no fluorescence due to excimers was detected, indicating that the rigidity of the spiro-linkage prevents strong intermolecular interactions. The absolute photoluminescence quantum yields (Φ_{PL}) of the neat films of asymmetric SSFs were measured using an integrating sphere[33] and are given in Table 2. The absolute PL quantum yields were found to be quite high between 0.31 and 0.54 ($\lambda_{ex} = 325$ nm), suggesting that asymmetric SSFs show an aggregation-induced emission (AIE) in the solid state. The enhancement of the absolute PL quantum yield ($\Phi_{PL} = 0.54$) for asymmetric BPhSSF **9c** is a direct result of both the unusually high PL quantum yield of the silole as an AIE active material and the incorporation of the highly fluorescent biphenyl moiety on the silole ring.

Electrochemical Properties. The electrochemical properties of asymmetric SSFs were characterized using cyclic voltammetry (CV) versus Ag/AgCl with a ferrocene/ferrocenium internal standard. An estimate of their HOMO and LUMO energy levels was deduced from their redox potentials. Figure 4 shows cyclic voltammograms of the three asymmetric SSFs that undergo single reduction and single oxidation; both processes are chemically irreversible. Irreversible reduction may be due to the extremely short lifetime (on the order of several nanoseconds) of the corresponding radical anions that cannot be detected on the CV time scale.[34] Similar irreversible redox processes have been observed in many silole derivatives, suggesting that the redox properties of 9-silafluorenes are governed by the modified silole ring of the asymmetric SSFs. When sweeping cathodically, BPhSSF **9c** displayed a cathodic peak potential (E_{pc}) of -2.70 V, whereas PySSF **9b** showed a smaller reduction peak potential of -2.45 V, reflecting the electron-accepting nature of the pyridyl group in PySSF **9b**.

Table 3. Electrochemical Properties of Asymmetric Spirosilabifluorenes

compd	E_{onset}^{ox} (V)[a]	E_{onset}^{red} (V)[a]	E_{HOMO} (eV)[b]	E_{LUMO} (eV)[b]	E_g (eV)
PhSSF	1.09	–	−5.79	–	–
PySSF	1.17	−2.24	−5.87	−2.46	3.41
BPhSSF	1.11	−2.42	−5.81	−2.28	3.53
Alq_3	0.73[c]	−2.30[c]	−5.53	−2.50	3.03

[a] Determined from cyclic voltammetry in CH_3CN:THF [9:1 (v/v)] using Ag/AgCl (0.01 M) as a reference electrode at a scan rate of 100 mV/s. [b] HOMO and LUMO levels were determined using the following equations: E_{HOMO} (eV) $= -e(E_{onset}^{ox} + 4.8)$, E_{LUMO} (eV) $= -e(E_{onset}^{red} + 4.8)$. [c] Reference 36.

The electrochemical reduction process of PhSSF **9a** was not observed. Upon changing the substituents on the 9-silafluorene ring, all three asymmetric SSFs had similar anodic peak potentials (E_{pa}) of around 1.30 V, suggesting that the HOMO is primarily localized on the silafluorene and its energy level is not affected by the aryl substituents. The HOMO and LUMO levels for asymmetric SSFs were estimated on the basis of an oxidation potential of -4.8 eV (below the vacuum level) for the ferrocene/ferrocenium (Fc/Fc^+).[35] The onset potentials of oxidation and reduction for BPhSSF **9c** were determined to be 1.11 and -2.42 V, respectively (vs Ag/AgCl), corresponding to 1.01 and -2.52 V (vs Fc/Fc^+). Thus, the HOMO and LUMO levels for BPhSSF **9c** are estimated to be -5.81 and -2.28 eV, respectively. Similarly, the HOMO and LUMO levels for PySSF **9b** are -5.87 and -2.46 eV, respectively. In Figure 4, the reduction CV curve of PySSF **9b** shows a relatively low (i.e. large electronic affinity) onset potential (-2.34 V vs Fc/Fc^+), maintaining a wide (HOMO−LUMO) electrochemical band gap (3.41 eV). Hence PySSF **9b** may be a good candidate as an electron transporter as well as an efficient hole blocker. Its reduction potential is nearly identical to that of Alq_3 (ca. -2.30 V vs Fc/Fc^+),[36] the most commonly used electron-transporting material in OLEDs but considerably larger than that of the air-stable electron-transporting material PyPySPyPy (-2.05 V vs Fc/Fc^+).[37] The estimated electrochemical band gaps of asymmetric SSFs (3.4−3.5 eV) are consistent with the measured optical band gaps (3.3−3.4 eV) listed in Table 3.

Conclusion

In summary, we have described a facile route for the synthesis of highly fluorescent asymmetrically aryl-substituted spirosilabifluorenes. The materials exhibited excellent thermal and morphological stability. The measured high glass transition temperatures ($T_g = 203-228$ °C) were attributed to the increased rigidity of the spiro-linked orthogonal bifluorene moieties. The absorbance spectra of the asymmetric spirosilabifluorenes showed significant bathochromic shifts relative to those of their carbon analogues as a result of the effective $\sigma^*-\pi^*$ conjugation between the σ^* orbital of the exocyclic Si−C bond and the π^* orbital of the oligoarylene fragment. All of the asymmetric spirosilabifluorenes were found to exhibit intense violet-blue

(33) Mattoussi, H.; Murata, H.; Merritt, C. D.; Iizumi, Y.; Kido, J.; Kafafi, Z. H. *J. Appl. Phys.* **1999**, *86*, 2642.
(34) Moiseeva, A. A.; Rakhimov, R. D.; Beloglazkina, E. K.; Butin, K. P.; Nosov, K. S.; Lee, V. Y.; Egorov, M. P. *Russ. Chem. Bull. Int. Ed.* **2001**, *50*, 2071.
(35) Lee, S. H.; Jang, B.-B.; Tsutsui, T. *Macromolecules* **2002**, *35*, 1356.
(36) Anderson, J. D.; McDonald, E. M.; Lee, P. A.; Anderson, M. L.; Ritchie, E. L.; Hall, H. K.; Hopkins, T.; Mash, E. A.; Wang, J.; Padias, A.; Thayumanavan, S.; Barlow, S.; Marder, S. R.; Jabbour, G. E.; Shaheen, S.; Kippelen, B.; Peyghambarian, N.; Wightman, R. M.; Armstrong, N. R. *J. Am. Chem. Soc.* **1998**, *120*, 9646.
(37) Uchida, M. Private communication.

emission (λ_{PL} = 398−415 nm) with high solid-state photoluminescence quantum yields (30−55%), suggesting that they are excellent candidates as emissive materials in OLEDs and solid-state lasers. PySSF has a low-lying LUMO energy level (−2.46 eV) and a relatively wide electrochemical (HOMO−LUMO) band gap (3.41 eV). Further studies on the asymmetric SSFs and their incorporation as electroactive materials (violet-blue emitters and/or electron transporters) in OLEDs are in progress.

Acknowledgment. This work was financially supported by the Office of Naval Research.

Note Added after ASAP Publication: There were two typographical errors, one in ref 23 and one in footnote b of Table 3, in the version published on the Web June 7, 2005. The version published June 9, 2005 and the print version are correct.

JA042762Q